Generation and characterization of a lysosomally targeted, genetically encoded Ca^{2+}-sensor

Hannah V. McCUE[1], Joanna D. WARDYN[1], Robert D. BURGOYNE and Lee P. HAYNES[2]

The Physiological Laboratory, Department of Cellular and Molecular Physiology, Institute of Translational Medicine, University of Liverpool, Crown St, Liverpool L69 3BX, U.K.

Distinct spatiotemporal Ca^{2+} signalling events regulate fundamental aspects of eukaryotic cell physiology. Complex Ca^{2+} signals can be driven by release of Ca^{2+} from intracellular organelles that sequester Ca^{2+} such as the ER (endoplasmic reticulum) or through the opening of Ca^{2+}-permeable channels in the plasma membrane and influx of extracellular Ca^{2+}. Late endocytic pathway compartments including late-endosomes and lysosomes have recently been observed to sequester Ca^{2+} to levels comparable with those found within the ER lumen. These organelles harbour ligand-gated Ca^{2+}-release channels and evidence indicates that they can operate as Ca^{2+}-signalling platforms. Lysosomes sequester Ca^{2+} to a greater extent than any other endocytic compartment, and signalling from this organelle has been postulated to provide 'trigger' release events that can subsequently elicit more extensive Ca^{2+} signals from stores including the ER. In order to investigate lysosomal-specific Ca^{2+} signalling a simple method for measuring lysosomal Ca^{2+} release is essential. In the present study we describe the generation and characterization of a genetically encoded, lysosomally targeted, cameleon sensor which is capable of registering specific Ca^{2+} release in response to extracellular agonists and intracellular second messengers. This probe represents a novel tool that will permit detailed investigations examining the impact of lysosomal Ca^{2+} handling on cellular physiology.

Key words: cameleon, calcium, fluorescence resonance energy transfer (FRET), lysosome, sensor, signalling, targeting.

INTRODUCTION

Ca^{2+} signalling is ubiquitous within animal cells and has an impact upon all aspects of normal cellular physiology to some degree [1,2]. The utility of the Ca^{2+} ion in cell signalling events stems from the ability of cells to regulate precisely where and when Ca^{2+} signals are generated and terminated through the co-ordinated activity of families of proteins dedicated to controlling the release (Ca^{2+} channels) and clearance (Ca^{2+} pumps and exchangers) of Ca^{2+} to and from the cytosol [3]. The interplay of Ca^{2+}-releasing and clearance mechanisms generates diverse spatiotemporal Ca^{2+} signals that in turn drive distinct alterations in cellular physiology, largely through the activation of specific Ca^{2+}-sensing proteins [4,5]. Ca^{2+} entry into the cytosol is the initiating event in any Ca^{2+} signal and may occur either by the opening of plasma membrane Ca^{2+} channels [6] and influx of extracellular Ca^{2+} or by release of sequestered Ca^{2+} from intracellular organelles [7]. The most extensively studied intracellular Ca^{2+} depot is the ER (endoplasmic reticulum) which stores Ca^{2+} to millimolar concentrations and releases it through two classes of channel protein. The first ER Ca^{2+}-release channel to be identified was the IP$_3$R [IP$_3$ (inositol 1,4,5-trisphosphate) receptor] [8] which is activated following stimulation of cell-surface receptors coupled to the intracellular enzyme PLC (phospholipase C). Hydrolysis of the plasma membrane lipid PIP$_2$ (phosphatidylinositol 4,5-bisphosphate) by PLC liberates two second messengers, diacylglycerol (a protein kinase C activator) and IP$_3$ [9] which diffuses to the ER and activates Ca^{2+} release through its cognate receptor. The second class of ER

Ca^{2+}-release channel is the RyR (ryanodine receptor) [10] that is activated by cADPR (cADP ribose), a second messenger synthesized in mammals from NAD$^+$ by the multifunctional enzyme CD38 [11]. IP$_3$Rs and RyRs share structural and functional homology and both are large multi-domain ligand-gated channels that are additionally regulated by Ca^{2+} itself [12]. Ca^{2+} regulation of ER Ca^{2+} release or CICR (Ca^{2+}-induced Ca^{2+} release) [13] is thought to be critical to the propagation of regenerative Ca^{2+} spikes and global Ca^{2+} waves within cells. Cytoplasmic and ER Ca^{2+} appears to influence IP$_3$R and RyR activity, and this complex regulatory behaviour has led some to speculate that Ca^{2+} may in fact be the primary modulator of channel opening and that the specific ligands, IP$_3$ and cADPR, may act secondarily to affect channel sensitivity to Ca^{2+}. The role that Ca^{2+} signals generated at the ER by RyRs and IP$_3$Rs have to play in the control of key cellular pathways is well established in various experimental systems; however, a second intracellular Ca^{2+}-release pathway has now been discovered that is less well characterized but which exhibits some remarkable properties.

NAADP is a pyridine nucleotide that is synthesized and metabolized by the same family of CD38 enzymes responsible for the biosynthesis and turnover of cADPR [14,15]. NAADP is the most potent Ca^{2+}-mobilizing second messenger known and, through a series of elegant studies, has been shown to release Ca^{2+} specifically from non-ER acidic compartments within the endolysosomal system of cells [16–18]. An emerging theme in the study of Ca^{2+} signalling is that subcellular organelles distinct from the ER are also able to sequester Ca^{2+} to concentrations suitable for functional Ca^{2+}-signalling events [19]. Ca^{2+} uptake

by acidic stores is believed to be coupled to generation of a proton gradient by the bafilomycin-sensitive vacuolar ATPase, as treatment with this drug rapidly dissipates luminal Ca^{2+} from these organelles [18]. The NAADP-activated Ca^{2+}-release channel remained elusive until the discovery of a novel family of endolysosomal-specific membrane proteins designated the TPCs (two-pore channels) which share similarities with voltage-gated Ca^{2+} channels [20,21]. There are three TPC isoforms in most vertebrate species; however, in humans only TPC1 and TPC2 are present [22,23]. TPC1 localizes predominantly to endosomal compartments and TPC2 to lysosomes. It has been determined that, of the various endolysosomal compartments, lysosomes are capable of sequestering Ca^{2+} to the greatest extent and this is consistent with the more acidic luminal pH of this organelle and the importance of the proton gradient in permitting such compartments to concentrate Ca^{2+}. A number of cell-based and biochemical studies have now provided strong evidence that TPC proteins mediate responses to NAADP and act as Ca^{2+}-release channels from endolysosomal stores, although the precise mechanistic basis of this pathway remains to be fully described [14]. Evidence indicating the importance of NAADP release from lysosomes through TPC2 in a physiological setting has been provided from studies examining TPC2 loss of function in various tissues from a knockout mouse animal model [21] and analyses of RNAi (RNA interference)-mediated depletion of TPC2 in cellular systems [24]. The current model of lysosomal Ca^{2+}-release activity in the context of wider cellular Ca^{2+} signalling couples lysosomal compartments closely with ER Ca^{2+}-release activity and invokes the acidic stores as 'trigger' sites, Ca^{2+} release from which directly modifies Ca^{2+} dynamics at the ER to generate complex widespread Ca^{2+}-signalling events [25]. This model builds a new dimension into cellular Ca^{2+} signalling and permits an additional level of regulation of ER Ca^{2+} release to be exerted through NAADP-generating signalling pathways.

Lysosomes are the central catabolic organelle of the cell and are responsible for degrading a range of cellular materials including endocytosed cell-surface receptors and autophagocytosed cellular debris [26]. Lysosomes have functions beyond those of waste disposal and, in addition to their emerging status as Ca^{2+}-signalling platforms, can, for instance, act as membrane reservoirs during the Ca^{2+}-dependent process of plasma membrane wound healing [27]. In order to assess the role of lysosomal Ca^{2+} signalling in intact cells and during stimulation with endogenous agonists or during specific lysosomal activities (catabolism, membrane repair etc.), a simple means of measuring specific lysosomal-related Ca^{2+} signals is required. To this end, we describe in the present study the generation of a novel lysosomally targeted Ca^{2+}-sensitive FRET (fluorescence resonance energy transfer) probe consisting of the lysosomal-resident membrane protein LAMP1 (lysosome-associated membrane protein 1) [28] fused to the YCaM3.6 cameleon [29] (LAMP1–YCaM). We demonstrate that this genetically encoded ratiometric sensor efficiently targets, and detects Ca^{2+} in close proximity to, the cytoplasmic face of lysosomes. Using a series of specific protocols we show that LAMP1–YCaM expressed in HeLa cells responds to Ca^{2+} signals generated by extracellular application of the physiological agonist histamine. Furthermore we demonstrate that histamine responses persist in cells pretreated with the ER SERCA (sarcoplasmic/endoplasmic reticulum Ca^{2+}-ATPase) pump inhibitor TG (thapsigargin) to deplete ER-Ca^{2+} content. We also characterize LAMP1–YCaM responses to the vacuolar ATPase inhibitor bafilomycin A1 which depletes Ca^{2+} specifically from endolysosomal stores and to the lysosomal disrupting agent GPN (glycyl-1-phenylalanine 2-naphthylamide). Collectively the results of the present study

demonstrate that LAMP1–YCaM is capable of responding to a variety of intracellular Ca^{2+} signals including those originating from acidic compartments, including lysosomes. We provide further additional data to show that LAMP1–YCaM FRET can be imaged at the level of individual lysosomes over time scales of seconds and thus exhibits properties suitable for studies requiring high spatial and temporal resolution. This probe will be of use in a broad range of future studies examining lysosomal Ca^{2+} dynamics and will permit detailed studies regarding how lysosomal Ca^{2+} is able to influence both lysosomal-specific and wider cellular activities.

MATERIALS AND METHODS

Buffers and reagents

LC (low-Ca^{2+}) buffer is 20 mM Hepes (pH 7.4), 145 mM NaCl, 5 mM KCl, 1.3 mM $MgCl_2$, 1.2 mM NaH_2PO_4 and 10 mM glucose. HC (high-Ca^{2+}) buffer is as for LC buffer but supplemented with 3 mM $CaCl_2$. Intracellular buffer is 5 mM Hepes (pH 6.8), 131 mM KCl, 20 mM NaCl, 1 mM ATP and 1 mM $MgCl_2$. Ultrapure TG and ionomycin were obtained from Sigma. Bafilomycin A1 was obtained from AbCam. All other reagents were of analytical grade and obtained from Sigma or Merck.

Cloning of LAMP1–YCaM

pcDNA-YCaM3.6 was a gift from the laboratory of Professor A Miyawaki (RIKEN Brain Institute, Japan). A SacII restriction endonuclease site (underlined in the sequences below) was inserted in-frame and directly 5′ of the YCaM3.6 start ATG codon (italics in the sequence below) by site-directed mutagenesis (QuikChange®, Stratagene) using the following primer pair: sense, 5′-AGACCC**AAGCTT**GCGGCCC*CGCGGATG*GGTGA-GCAAGGGCGAG-3′; and antisense, 5′-CTCGCCCTTGCT-CACCAT*CCGCGGG*GGCCGC**AAGCTT**GGGTCT-3′. pcDNA-YCaM3.6 also contained a pre-existing HindIII restriction endonuclease site (shown in bold in the mutagenesis primer sequence above). The coding sequence of murine LAMP1 (GenBank® accession number NM_010684) was PCR-amplified from mouse brain first-strand cDNA using the following primers containing restriction endonuclease sites for subsequent subcloning: sense (HindIII), 5′-ATAT*AAGCTT*ACCATGGCG-GCCCCCGGCGCCCGGCGG-3′; and antisense (SacII), 5′-AT-ATC*CGCGGG*GATGGTCTGATAGCCGGCGTGAC-3′. LAMP1 PCR product and the mutated SacII-containing YCaM3.6 plasmid were digested with HindIII and SacII restriction endonucleases (New England Biolabs) and subsequently ligated with T4 DNA ligase (New England Biolabs) according to the manufacturer's protocol. Recombinant LAMP1–YCaM plasmids were confirmed by restriction analysis and automated sequencing (The Sequencing Service, University of Dundee, Dundee, U.K.).

HeLa cell culture and transfection

HeLa cells [30] were maintained in DMEM (Dulbecco's modified Eagle's medium) supplemented with 5% FBS (fetal bovine serum), 1% penicillin/streptomycin and 1% non-essential amino acids in a humidified atmosphere of 5% CO_2/95% air at 37°C. Cells were transiently transfected using Genejuice transfection reagent (Novagen) according to the manufacturer's instructions. For co-localization studies with exogenously and endogenously expressed proteins, cells (1×10^5) were plated on to 13 mm glass coverslips and transfected with 1 μg each of the indicated

constructs. For live-cell Ca^{2+}-imaging analyses, cells (5×10^5) were plated on to 30 mm glass-bottomed tissue culture dishes (Matek) and transfected with 3 μg of LAMP1–YCaM. All cells were maintained for 24–48 h post-transfection before fixation or live imaging.

Western blot analysis

HeLa cells (1×10^6 cells/well) were plated on to 24-well tissue culture trays and transfected with 1 μg of pcDNA-YCaM3.6, LAMP1–EYFP [enhanced YFP (yellow fluorescent protein)] or pcDNA-LAMP1-YCaM plasmid. At 24 h post-transfection cells were washed twice with PBS, lysed by the addition of 50 μl of dissociation buffer [125 mM Hepes (pH 6.8), 10 % (w/v) sucrose, 10 % (v/v) glycerol, 4 % SDS, 1 % 2-mercaptoethanol and 2 mM EDTA] and boiled for 5 min. Protein samples were resolved by 8–16 % gradient SDS/PAGE (Novex, Invitrogen) and transferred on to nitrocellulose filters for Western blotting by transverse electrophoresis. The YFP tag in each of the transfected constructs was detected with a monoclonal anti-GFP (green fluorescent protein) primary antibody (1:1000 dilution, JL-8 clone, Clontech). Immunoreactivity was detected after application of horseradish-peroxidase-conjugated goat anti-mouse secondary antibody (1:400 dilution, Sigma) and visualized using ECL (enhanced chemiluminescence) reagents.

Immunofluorescence

HeLa cells plated on to 13 mm glass coverslips as described above were washed three times with PBS and fixed with PBS containing 4 % (v/v) formaldehyde for 6 min at room temperature (25 °C). Cells were washed twice with PBS and then permeabilized by incubation with PBS containing 0.2 % Triton X-100 for 6 min at room temperature. Cells were washed three times in PBS and twice in blocking solution [PBS containing 5 % (w/v) BSA (FirstLink, UK)] before incubation with either polyclonal anti-TGN46 (*trans*-Golgi network 46; 1:250 dilution, Sigma) or anti-CD63 (1:200 dilution, Biodesign) in blocking solution overnight at 4 °C with agitation. Cells were washed three times with PBS and twice with blocking solution before incubation with Alexa Fluor® 568-conjugated anti-rabbit (TGN46) or Alexa Fluor® 594-conjugated anti-mouse (CD63) secondary antibody (1:500, Invitrogen) in blocking solution for 1 h at room temperature. Coverslips were washed three times with PBS, air-dried and mounted on to glass slides using Prolong Gold anti-fade glycerol (Invitrogen).

Confocal imaging

Imaging of fixed cells was performed using a Leica TCS-SP-MP fluorescent scanning confocal microscope (Leica Microsystems), with 63× oil-immersion objective, 16× line averaging, 200 mHz scanning speed and pinhole set to 1 Airy unit. ECFP [enhanced CFP (cyan fluorescent protein)] present in LAMP1–YCaM was imaged by excitation at 405 nm and emission fluorescence collection between 450 and 490 nm. mCherry-tagged marker constructs and Alexa Fluor® 594-labelled endogenous proteins were imaged with excitation by a 594 nm laser line and emission fluorescence collection between 610 and 670 nm. Images were exported in .TIFF format and processed using the Corel graphics suite. In experiments monitoring LAMP1–YCaM FRET in live cells, transfected cells were used 24–48 h post-transfection. For perfusion experiments, cells plated on to 30 mm glass-bottomed tissue culture dishes (Matek), were inserted into an

aluminium cell perfusion holder maintained at room temperature. All perfusion solutions were equilibrated to room temperature before use and fed through a gravity flow apparatus. FRET data were collected by exciting the ECFP portion of LAMP1–YCaM with a 405 nm laser line and simultaneous collection of emitted fluorescence between 450 and 490 nm (ECFP) and 520 and 570 nm (EYFP). Images were collected at a rate of 12 frames/min (with 2× line averaging), 400 MHz scan speed and 63× water-immersion objective with maximum diameter pinhole. Regions of interest typically encompassing groups of LAMP1–YCaM-positive organelles were selected post-capture using Leica LAS software and numerical raw fluorescence intensity data exported as text files for analysis with Excel (Microsoft) and Origin 8.0 Professional (Origin Lab). All data were background-corrected (a region of interest in the same field of view that was devoid of cells was selected as background) and the FRET ratio of YFP/CFP emission intensity was calculated and plotted as a function of time.

RESULTS

Expression and subcellular localization of LAMP1–YCaM in HeLa cells

We first examined expression levels of the soluble cameleon protein YCaM3.6 along with LAMP1–EYFP and LAMP1–YCaM in HeLa cells by Western blotting with an antibody directed towards the YFP tag present in all three proteins (Figure 1). YCaM3.6 is a complex fusion cassette comprising ECFP–calmodulin–M13 peptide–EYFP with an approximate molecular mass of 70 kDa. LAMP1 fused to EYFP alone (LAMP1–EYFP) is also predicted to have a molecular mass of ∼ 70 kDa; however, the apparent molecular mass of this protein is higher than predicted as can be judged by comparison of the YCaM3.6 immunoreactive band with that of LAMP1–EYFP (Figure 1). This discrepancy is explained by the extensive glycosylation of LAMP1 protein, a prominent feature of all lysosomal membrane proteins and key to their protection from proteases of the lysosome lumen. LAMP1–YCaM has a predicted molecular mass of ∼ 113 kDa and there is a clear single immunoreactive band migrating above the 97 kDa molecular mass marker on SDS/PAGE for this protein (Figure 1). This analysis demonstrates that LAMP1–YCaM is expressed in HeLa cells, appears at the correct molecular mass on SDS/PAGE and exhibits no obvious signs of proteolytic degradation. Furthermore, each of the constructs tested exhibited broadly similar levels of expression, indicating that there is no significant difference in LAMP1–YCaM protein levels when compared directly with related fusion proteins (Figure 1).

With the knowledge that LAMP1–YCaM protein expresses efficiently in HeLa cells we next examined the subcellular localization of the protein in the same cell type. LAMP1–YCaM ECFP fluorescence was visualized in these studies and localization was compared with co-transfected markers for known cellular organelles (Figures 2A–2D). Extensive co-localization was observed with LAMP1 fused to mCherry to numerous punctate structures distributed throughout the cytosol (LAMP1-mCh, Figure 2A). Similarly extensive co-localization was also observed with the endo-lysosomal marker TPC2 fused to mCherry to punctate structures of various sizes throughout the cytosol (mCh-TPC2, Figure 2B). Partial co-localization was observed with the autophagosomal/autophagolysosomal membrane marker LC3β fused to mCherry (mCh-LC3β, Figure 2C), and no co-localization was observed with the early-endosome-specific marker Rab5a fused to mCherry (mCh-Rab5a, Figure 2D). Similarly, no co-localization was observed between
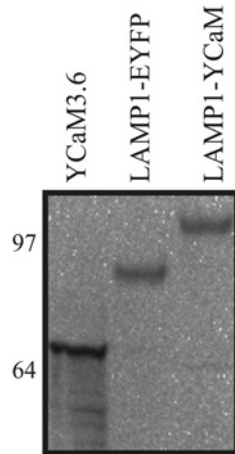
Figure 1   Verification of LAMP1–YCaM expression in HeLa cells by Western blot analysis

HeLa cells were transfected for 24 h with YCaM3.6, LAMP1–EYFP and LAMP1–YCaM, lysed and proteins were resolved by SDS/PAGE before Western blotting with an anti-GFP antibody which recognizes the EYFP tag present in all three constructs. Immunoreactive bands are present for each protein and at the correct molecular masses. Molecular mass markers are shown on the left-hand side for 64 kDa and 97 kDa protein standards.

LAMP1–YCaM and endogenous TGN46, a marker of the *trans*-Golgi network (Figure 2E).

In order to eliminate the possibility that LAMP1–YCaM localization was simply coincidental with lysosomal/late-endosomal markers we performed *z*-stack reconstructions of HeLa cells transfected with LAMP1–YCaM and immunostained with an antibody directed towards endogenous CD63, a marker of late-endosomes/lysosomes (Figure 3A). Three-dimensional reconstruction of the acquired image stacks confirmed that all CD63-positive structures were co-labelled by LAMP1–YCaM (Figure 3B and Supplementary Movie S1 at http://www.biochemj.org/bj/449/bj4490449add.htm).

LAMP1–YCaM as a probe of intracellular Ca^{2+}-release events

Responses to the extracellular agonist histamine

We first wanted to test whether LAMP1–YCaM was capable of responding to intracellular Ca^{2+} fluxes generated by agonists known to mobilize Ca^{2+} in HeLa cells [31]. In initial studies we utilised histamine as a Ca^{2+}-releasing extracellular agonist in intact cell experiments to assess the sensitivity of LAMP1–YCaM (Figure 4). Application of histamine elicited robust increases in FRET output from the cameleon construct, consistent with an elevation in cytosolic Ca^{2+} in close proximity to the lysosomal surface (Figure 4A). These responses were oscillatory in nature and the magnitude of each oscillatory FRET response decreased progressively in LC external buffer. In HeLa cells, histamine has previously been shown to liberate ER Ca^{2+} through generation of the second messenger IP_3 [32]. There is also evidence that histamine is capable of generating NAADP directly in some cell types [33], and we probed the possible existence of such a pathway in HeLa cells in related experiments. In this protocol, cells were first perfused in HC buffer to permit loading of internal stores (HeLa cell responses were highly variable and inclusion of a loading step with HC buffer was found to maximize signal-to-noise in many of our assays). Cells were then switched back to LC buffer before perfusion with the SERCA pump inhibitor TG [34] to first deplete ER Ca^{2+} before perfusion with histamine
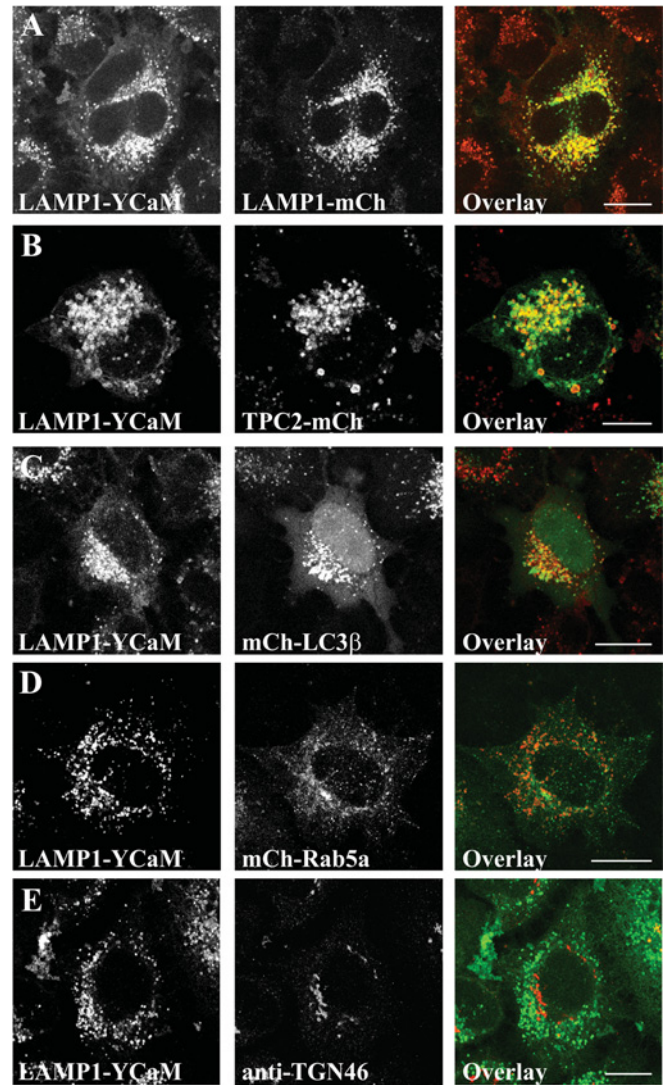
Figure 2   Localization of LAMP1–YCaM in HeLa cells

(**A–D**) HeLa cells were transfected with LAMP1–YCaM (green) along with plasmids encoding proteins specific for endolysosomal compartments [LAMP1-mCh (red, **A**), TPC2-mCh (red, **B**)], autophagosomes/autophagolysosomes [mCh-LC3β (red, **C**)] and early-endosomes [mCh-Rab5a (red, **D**)]. (**E**) Cells transfected with LAMP1–YCaM (green) were also fixed and immunostained with an antibody directed towards the endogenous *trans*-Golgi network-specific marker TGN46 (anti-TGN46, red). Co-localization of fluorescence channels appears yellow in overlay images. Scale bars = 10 μm.

(Figure 4B). TG responses were relatively slow to develop and exhibited an average FRET response that was $27.01 \pm 1.06\%$ (mean $\pm$ S.E.M.) of the maximal response induced in response to incubation with HC external buffer ($n = 14$ cells from three independent experiments). In the same experiments we were able to observe reproducible post-TG treatment histamine-induced FRET responses that were on average $40.32 \pm 5.81\%$ (mean $\pm$ S.E.M.) of the maximal FRET signal observed in response to HC buffer application. Interestingly, these histamine responses failed to exhibit oscillatory behaviour and instead gave rise to a single short-lived Ca^{2+} spike. It was not possible to test the well-characterized antagonist of NAADP signalling Ned-19 [35] in these experiments as it was found to fluoresce strongly in the blue region of the visible spectra and therefore interfered with the emission spectra of the CFP tag in LAMP1–YCaM. Consistent with these observations, treatment of LAMP1–YCaM-transfected
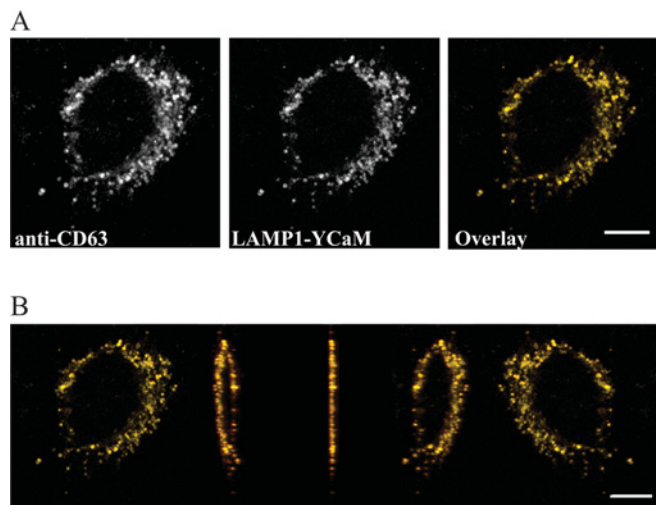
Figure 3   Co-localization of LAMP1–YCaM with endogenous CD63 and a three-dimensional reconstruction of z-series image stacks

(**A**) HeLa cells were transfected with LAMP1–YCaM (green) and immunostained for endogenous endolysosomal CD63 (red). Co-localization appears yellow in overlay images. (**B**) Serial confocal sections from the same cell represented in (**A**) were acquired and used to reconstruct a three-dimensional rendition of LAMP1–YCaM (green) and endogenous CD63 (red) localization. Five alternative viewing angles are represented from the total image stack composed of 50 separate confocal sections that was reconstructed and rotated through 180°. Co-localization of fluorescence channels appears yellow in the overlay images. Scale bars = 10 μm.

cells with TG followed by bafilomycin A1 before the application of histamine (Figure 4C) inhibited any detectable histamine-evoked FRET responses in 85 % of cells imaged ($n = 20$ cells from three independent experiments).

Responses to lysosomal-disrupting agents and direct application of intracellular second messengers

In order to investigate additional applications of LAMP1–YCaM in measurements of intracellular Ca^{2+} signals we next examined responses to both the lysosome-disrupting agent GPN and the ER Ca^{2+}-mobilizing agonist IP$_3$ (Figure 5). GPN [36] generated reproducible FRET responses from LAMP1–YCaM (Figure 5A). These responses occurred over a timescale of minutes, consistent with the mode of action of this compound in osmotic swelling and eventual lysis of lysosomes.

In order to test the ability of LAMP1–YCaM to respond to direct application of a key Ca^{2+}-mobilizing intracellular second messenger we used a well-characterized digitonin cell-permeabilization protocol [37] to permit direct access of IP$_3$ to the cell cytosol. This strategy bypasses the requirement for an extracellular agonist and can conceivably be used to accurately study cellular responses to a vast array of signalling molecules. IP$_3$-generated reproducible LAMP1–YCaM FRET responses (Figure 5B, representative data) that occurred with faster kinetics than observed with TG treatment (Figure 4) and this is probably due, in part, to the additional time required for TG to traverse the plasma membrane and diffuse to the ER ($n = 16$ similar cell responses from three independent experiments, where 23 LAMP1–YCaM-positive cells were imaged in total).

Visualizing LAMP1–YCaM FRET at the level of individual organelles

In addition to using the LAMP1–YCaM construct to monitor simultaneous Ca^{2+} release from populations of lysosomes, we
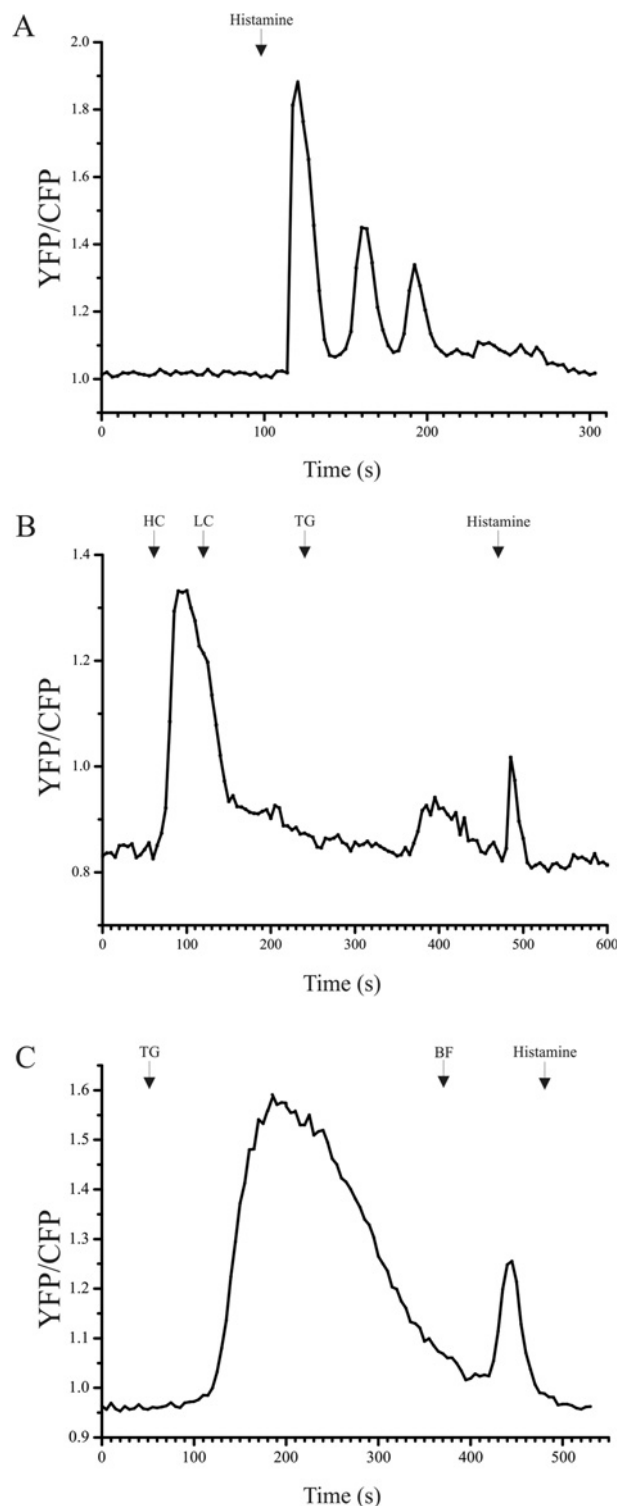
Figure 4   LAMP1–YCaM FRET responses in intact HeLa cells in response to histamine, TG and bafilomycin A1

(**A**) HeLa cells transfected with LAMP1–YCaM were perfused with LC buffer and perfusion was changed to LC buffer containing 100 μM histamine at the indicated time. FRET output from LAMP1–YCaM is calculated as the ratio of YFP/CFP fluorescence and plotted against time. This is a representative single-cell response taken from eight cells acquired over three independent experiments where oscillatory responses to histamine were observed. (**B**) HeLa cells transfected with LAMP1–YCaM were perfused with HC buffer to permit loading of internal stores then switched to LC buffer to permit FRET output to return to basal levels. At the indicated times, cells were perfused with 2 μM TG in LC buffer followed by 100 μM histamine in LC buffer. FRET output from LAMP1–YCaM is calculated as the ratio of YFP/CFP fluorescence and plotted against time.
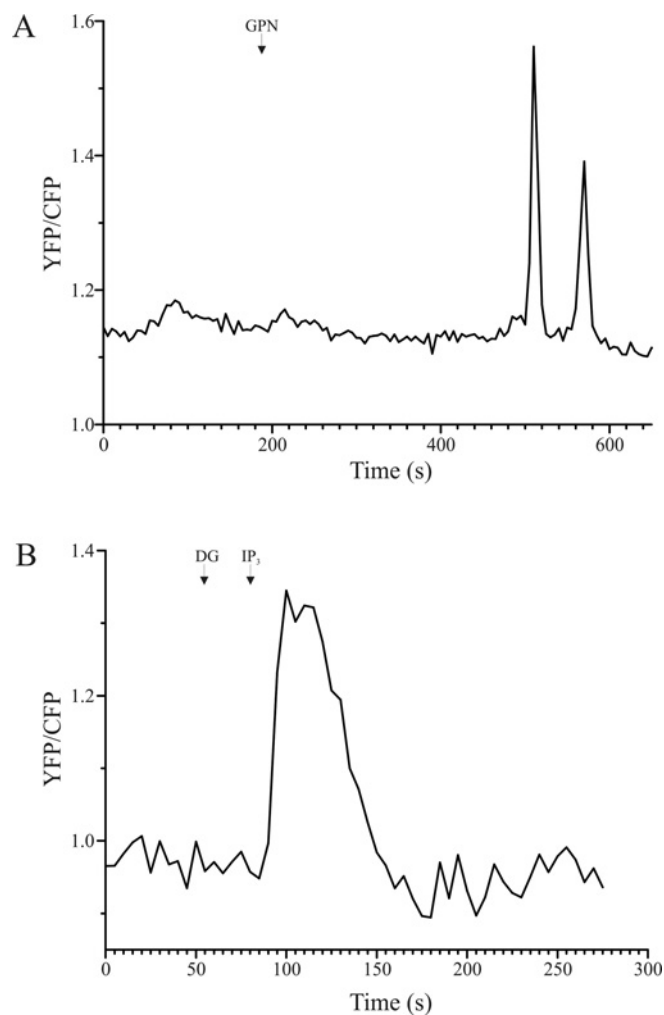
Figure 5   LAMP1–YCaM responses to lysosome disruption with GPN and Ca^{2+} mobilization from the ER through direct application of IP$_3$

(**A**) HeLa cells transfected with LAMP1–YCaM were perfused in LC buffer then switched to LC buffer containing 500 μM GPN at the indicated time point. This trace is a representative response from a total of three independent cell responses. FRET output from LAMP1–YCaM is calculated as the ratio of YFP/CFP fluorescence and plotted against time. (**B**) HeLa cells transfected with LAMP1–YCaM were perfused with LC buffer then permeabilized by perfusion with 40 μM digitonin (DG) in intracellular buffer. The perfusion solution was switched to intracellular buffer containing 10 μM IP$_3$ at the indicated time point. This is a representative response from a total of 16 similar cell responses imaged over three independent experiments ($n = 23$ LAMP1–YCaM-expressing cells in total). FRET output from LAMP1–YCaM is calculated as the ratio of YFP/CFP fluorescence and plotted against time.

also assessed the utility of this probe to measure Ca^{2+} release at the single-organelle level (Figure 6 and Supplementary Movie S2 at http://www.biochemj.org/bj/449/bj4490449add.htm). HeLa cells were incubated in HC buffer (Figure 6A, -ionomycin) and then switched to HC buffer supplemented with 1 μM ionomycin (Figure 6A, + ionomycin) to permit elevation of the

This is a representative single-cell response taken from a total of 14 cell responses acquired over three independent experiments. (**C**) HeLa cells transfected with LAMP1–YCaM were perfused in LC buffer then switched to LC buffer containing 2 μM TG at the indicated time point. The perfusion solution was subsequently switched to LC buffer containing 500 nM bafilomycin A1 (BF) and then to LC buffer containing 100 μM histamine. This trace is a representative response from a total of 17 similar cell responses acquired from three individual experiments ($n = 20$ LAMP1–YCaM-expressing cells in total). FRET output from LAMP1–YCaM is calculated as the ratio of YFP/CFP fluorescence and plotted against time.
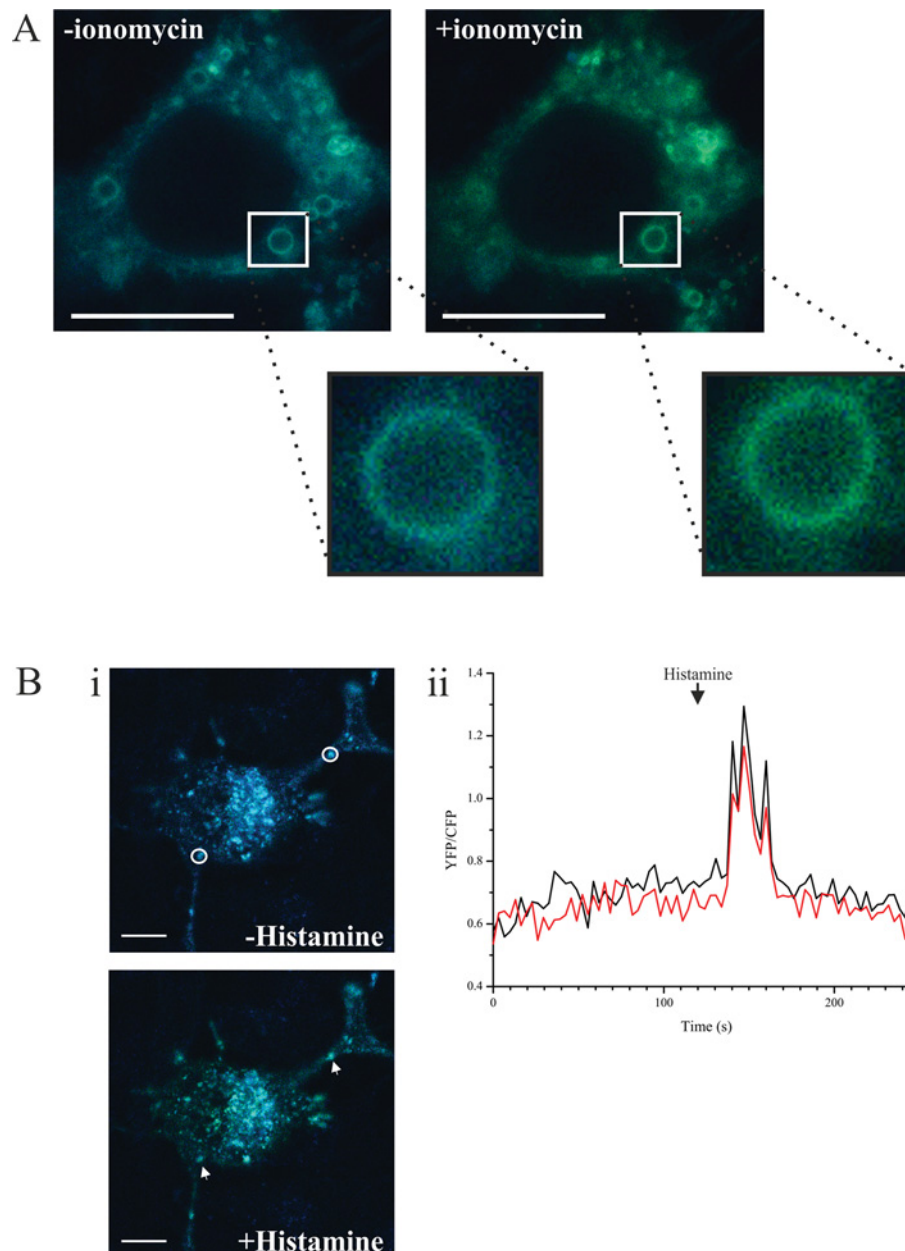
cytosolic Ca^{2+} concentration. A single LAMP1–YCaM-positive organelle from a representative HeLa cell has been selected and magnified to highlight the FRET response of LAMP1–YCaM at the single-organelle level. Before ionomycin treatment and with CFP excitation with a 405 nm laser line, the LAMP1–YCaM fluorescence signal was blue, consistent with a lack of FRET under resting conditions. Post-ionomycin treatment the same organelle exhibited a green fluorescence output (a mixture of CFP and YFP emission) consistent with induction of FRET between the CFP and YFP portions of LAMP1–YCaM upon elevation of cytosolic Ca^{2+}. In related experiments we also examined single-organelle FRET responses to application of extracellular histamine (Figure 6B). A representative HeLa cell is shown from such an experiment where two LAMP1–YCaM-positive organelles at distinct locations were monitored for alterations in FRET. In the absence of histamine (Figure 6Bi, -Histamine) fluorescence output from LAMP1–YCaM at these two vesicular structures was blue, consistent with CFP fluorescence and no FRET to YFP. On application of 100 μM histamine (Figure 6Bi, + Histamine), LAMP1–YCaM fluorescence in the selected regions appeared green, indicating FRET between the CFP and YFP components of LAMP1–YCaM. The FRET ratio (YFP/CFP) plot against time (Figure 6Bii) clearly demonstrates induction of FRET in LAMP1–YCaM at these two vesicular structures.

DISCUSSION

Ca^{2+} signalling underpins numerous essential physiological processes, many of which have been studied in detail over the last 40 years. Understanding precisely how Ca^{2+} signals are generated and the mechanisms by which they subsequently modulate unique alterations in specific cellular pathways is of fundamental importance in modern cell biology. Defects in Ca^{2+} homoeostasis play a role in multiple human disease pathologies [38–41] and, although the mammalian Ca^{2+}-signalling apparatus itself appears to exhibit resilience to damage of single components (most probably through functional redundancy), defects in this machinery can also lead directly to disease [42].

Much is known regarding the generation and propagation of Ca^{2+} signals by dedicated Ca^{2+}-channel proteins distributed to either the plasma membrane or ER. Complex regenerative cytosolic Ca^{2+} signals often occur through the process of CICR and this relies on the activity of ER-resident IP$_3$Rs and RyRs [3]. The ligands for these channels are the intracellular second messengers IP$_3$ and cADPR respectively. The discovery of a second NAD-related molecule, NAADP, as the most potent Ca^{2+}-mobilizing agent characterized to date hinted at further complexity in the Ca^{2+}-signalling system. NAADP was shown to liberate Ca^{2+} from non-ER cellular organelles that have subsequently been defined as acidic compartments of the late-endocytic/lysosomal pathway [21]. Lysosomes have, in recent years, been demonstrated to exhibit activities beyond a purely catabolic function, including acting as membrane donors [27] and as Ca^{2+} stores [43,44]. Further dissection of the lysosomal Ca^{2+}-signalling apparatus has demonstrated that these organelles harbour the necessary Ca^{2+}-uptake and -release components to act as autonomous signalling platforms [45]. The interplay between NAADP-driven Ca^{2+} release and subsequent generation of Ca^{2+} signals at the ER has led to the formulation of the 'trigger' hypothesis whereby NAADP-gated release of Ca^{2+} from endolysosomal stores exerts a stimulatory effect upon IP$_3$/RyR-triggered release of Ca^{2+} from the ER. In this way, NAADP-generating cell signalling pathways are able to impart additional regulation on cellular Ca^{2+}-signalling events [19]. Interestingly,

Figure 6   LAMP1–YCaM FRET responses visualized on single organelles

(**A**) HeLa cells transfected with LAMP1–YCaM were incubated in LC buffer in the absence of ionomycin (-ionomycin) and subsequently perfused in HC buffer supplemented with 1 μM of the Ca^{2+} ionophore ionomycin to elevate cytosolic Ca^{2+} (+ionomycin). A representative cell is depicted. LAMP1–YCaM fluorescence output in the absence of ionomycin using CFP excitation with a 405 nm diode laser appeared blue due to the absence of FRET between CFP and YFP in LAMP1–YCaM. On application of ionomycin, LAMP1–YCaM fluorescence emission appeared green (a mixture of CFP and YFP emission spectra) due to induction of FRET. A single LAMP1–YCaM-positive organelle has been selected and magnified to illustrate the visible induction of FRET at this level of spatial resolution. (**B**) HeLa cells transfected with LAMP1–YCaM were loaded in HC buffer then switched to LC buffer to permit FRET to return to basal levels (i, -Histamine). A representative cell is depicted where FRET was monitored at two LAMP1–YCaM-positive organelles (i, white circles in -Histamine and white arrows in +Histamine). Fluorescence output in the absence of histamine using CFP excitation with a 405 nm diode laser appeared blue due to the absence of FRET between CFP and YFP in LAMP1–YCaM. On application of 100 μM histamine (i, +Histamine) LAMP1–YCaM fluorescence emission appeared green (a mixture of CFP and YFP emission spectra) due to induction of FRET. FRET responses from the two selected LAMP1–YCaM-positive organelles calculated as the YFP/CFP ratio were plotted against time (ii). Scale bars = 10 μm.

defects in lysosomal Ca^{2+} handling have also been implicated in the pathogenesis of numerous genetically inherited lysosomal storage diseases [45,46] and, therefore, fully understanding the dynamics of Ca^{2+} signalling from these compartments is of tangible importance.

A potential hurdle to studying lysosomal Ca^{2+} signals stems from the fact that, although these organelles sequester Ca^{2+} to high concentrations, the total amount of luminal Ca^{2+} within each lysosome is small compared, for example, with the extensive volume of the continuous ER lumen. Therefore each lysosomal release event may be undetectable above background noise with conventional diffusely distributed cytosolic Ca^{2+} indicators. Indeed, in a previous study, TPC2 overexpression was required before NAADP responses could be reliably detected with the cytosolic indicator fluo-3 [15]. With these facts in mind we started the present study by constructing a lysosomally targeting

Ca^{2+}-sensing cameleon plasmid (LAMP1–YCaM), whereby the short cytoplasmic C-terminal tail of the lysosomal resident type-I membrane protein LAMP1 was fused, in-frame, to YCaM3.6 [29,47]. The rationale behind this approach was to use an intramolecular FRET construct that has high intrinsic FRET efficiency (YCaM3.6 has a dynamic range of 560 % [29]) and concentrate it, through fusion to a resident lysosomal membrane protein, in close proximity to the cytoplasmic face of the lysosomal membrane. In theory such a probe should be ideally placed to sense Ca^{2+}-release events directly from the lysosome itself, and would exhibit substantially higher signal-to-noise characteristics than a freely diffusible cytosolic Ca^{2+} indicator. In a previous study, a similar approach was successfully taken to examining secretory granule Ca^{2+} signalling by fusion of the YCaM2 cameleon probe to the dense core vesicle protein phogrin [48].

In initial analyses, we assessed the proper expression and localization of LAMP1–YCaM in HeLa cells. This genetically encoded Ca^{2+} probe would only be of experimental use in further functional studies if it was stable, correctly folded, and maintained the ability to efficiently express and target to lysosomal compartments. We demonstrated that LAMP1–YCaM was expressed efficiently and localized extensively with lysosome/late-endosome markers, but not with early-endosomal or *trans*-Golgi markers. This co-localization was confirmed using three-dimensional reconstructions of image stacks in cells expressing LAMP1–YCaM and immunostained for the endolysosomal-specific membrane protein CD63.

With the knowledge that LAMP1–YCaM was stable, expressed appropriately and targeted as predicted, we next examined its responses to various stimuli designed to liberate Ca^{2+} from intracellular stores. We first examined whether the LAMP1–YCaM FRET signal was detectable in response to application of endogenous agonists known to generate cytosolic Ca^{2+} transients in intact HeLa cells [31]. As has been previously observed, histamine evoked a series of repetitive oscillations in cytosolic Ca^{2+} which were detected by LAMP1–YCaM. These oscillations decreased progressively in amplitude when cells were perfused in LC buffer, consistent with emptying of intracellular stores which were then unable to refill through the store-operated Ca^{2+} entry route [49]. To investigate this pathway further we pre-treated cells with the ER SERCA pump inhibitor TG to deplete ER Ca^{2+} content. In these cells, subsequent application of histamine generated a single short-lived Ca^{2+} transient in contrast with the oscillatory behaviour observed in the absence of TG. Histamine has been shown to couple to an NAADP-generating pathway in endothelial cells [33] and our interesting observations are consistent with histamine similarly releasing Ca^{2+} from a non-ER intracellular store in HeLa cells. That this Ca^{2+} release lacks oscillatory behaviour is consistent with the properties of the endolysosomal Ca^{2+}-release machinery which, unlike that present on the ER, is insensitive to Ca^{2+} and so there is no CICR-like phenomenon.

Since the LAMP1–YCaM construct responded to TG treatment, this demonstrates its capacity to detect global increases in cytosolic Ca^{2+}. That these responses exhibited a lag not observed when using cytosolic Ca^{2+} indicators [50] is consistent with the time taken for diffusion of Ca^{2+} from release sites at the ER to the lysosome. Our TG-histamine sequential-treatment experiments on intact cells suggests that the cameleon can probably register endolysosomal-specific release events. Consistent with our TG responses, LAMP1–YCaM also detected Ca^{2+} signals following cell permeabilization and direct application of the ER-Ca^{2+}-mobilizing agonist IP$_3$. The ability to directly introduce intracellular second messengers and specific antagonists to

manipulate Ca^{2+}-signalling pathways in this manner extends the range of potential applications for LAMP1–YCaM in studies of lysosomal Ca^{2+} signalling. This is of particular importance for cell-impermeant molecules for which caged or esterified forms are unavailable. In order to accurately determine the role of Ca^{2+} in aspects of lysosomal and wider cellular function it is likely that future studies will include analysis of single-organelle dynamics. In the present study we provide data indicating that LAMP1–YCaM exhibits the requisite spatiotemporal characteristics as a Ca^{2+} sensor to permit such investigations and demonstrate visible measurable alterations in FRET output at the surface of single organelles in response to direct elevation of cytosolic Ca^{2+} and to a physiologically relevant Ca^{2+}-mobilizing extracellular ligand.

In the present paper we report the generation and characterization of the novel lysosomally targeted cameleon Ca^{2+} probe LAMP1–YCaM. We show that this genetically encoded sensor accurately and sensitively responds to both global and lysosome-specific Ca^{2+} signals, and outline simple protocols for studying endogenous lysosomal Ca^{2+} dynamics in a widely used model cell system. Lysosomal Ca^{2+} signalling is an area of Ca^{2+} biology that is gaining increasing attention due to the characterization of lysosomes as important Ca^{2+} signalling platforms. In future studies it will be interesting to examine how lysosomal Ca^{2+} transients are triggered, under what circumstances these events couple to more extensive signalling activity at the ER and how lysosomal Ca^{2+} signals are linked to specific aspects of lysosomal function. During the preparation of this manuscript a paper was published detailing the generation of a genetically encoded and lysosomally targeted Ca^{2+} sensor based upon GCaM single-wavelength Ca^{2+}-sensor technology [51,52]. LAMP1–YCaM has the additional advantage of being a ratiometric indicator and it would therefore be possible to calibrate the probe such that detailed information regarding the precise magnitude of lysosomal Ca^{2+} signals could be derived [53]. The ratiometric nature of LAMP1–YCaM is similarly advantageous in live-cell studies where cell movement might otherwise interfere with fluorescence imaging. This is clearly an important consideration when imaging Ca^{2+} responses on organelles that are highly dynamic, such as lysosomes (Supplementary Movie S2), where nevertheless we were able to demonstrate single-organelle-associated changes in Ca^{2+} concentration with LAMP1–YCaM. In conclusion we believe that LAMP1–YCaM represents a novel and powerful tool for studies of lysosomal Ca^{2+} signalling which will be of wide interest to researchers in this emerging area of cell biology.

AUTHOR CONTRIBUTION

FUNDING

REFERENCES

1   Berridge, M. J., Bootman, M. D. and Roderick, H. L. (2003) Calcium signalling: dynamics, homeostasis and remodelling. Nat. Rev. Mol. Cell Biol. **4**, 517–529

2   Berridge, M. J., Lipp, P. and Bootman, M. D. (2000) The versatility and universality of calcium signalling. Nat. Rev. Mol. Cell Biol. **1**, 11–21

3   Bootman, M. D., Collins, T. J., Peppiatt, C. M., Prothero, L. S., MacKenzie, L., De Smet, P., Travers, M., Tovey, S. C., Seo, J. T., Berridge, M. J. et al. (2001) Calcium signalling: an overview. Semin. Cell Dev. Biol. **12**, 3–10

4   Burgoyne, R. D. and Weiss, J. L. (2001) The neuronal calcium sensor family of Ca^{2+}-binding proteins. Biochem. J. **353**, 1–12

5   Burgoyne, R. D. (2007) Neuronal calcium sensor proteins: generating diversity in neuronal Ca^{2+} signalling. Nat. Rev. Neurosci. **8**, 182–193

6   Turner, R. W., Anderson, D. and Zamponi, G. W. (2011) Signaling complexes of voltage-gated calcium channels. Channels (Austin) **5**, 440–448

7   Iino, M. (1999) Dynamic regulation of intracellular calcium signals through calcium release channels. Mol. Cell. Biochem. **190**, 185–190

8   Mikoshiba, K. (2007) IP_3 receptor/Ca^{2+} channel: from discovery to new signaling concepts. J. Neurochem. **102**, 1426–1446

9   Michell, R. H. (1992) Inositol lipids in cellular signalling mechanisms. Trends Biochem. Sci. **17**, 274–276

10 Lanner, J. T., Georgiou, D. K., Joshi, A. D. and Hamilton, S. L. (2010) Ryanodine receptors: structure, expression, molecular details, and function in calcium release. Cold Spring Harbor Perspect. Biol. **2**, a003996

11 Malavasi, F., Deaglio, S., Funaro, A., Ferrero, E., Horenstein, A. L., Ortolan, E., Vaisitti, T. and Aydin, S. (2008) Evolution and function of the ADP ribosyl cyclase/CD38 gene family in physiology and pathology. Physiol. Rev. **88**, 841–886

12 Seo, M. D., Velamakanni, S., Ishiyama, N., Stathopulos, P. B., Rossi, A. M., Khan, S. A., Dale, P., Li, C., Ames, J. B., Ikura, M. and Taylor, C. W. (2012) Structural and functional conservation of key domains in InsP₃ and ryanodine receptors. Nature **483**, 108–112

13 Roderick, H. L., Berridge, M. J. and Bootman, M. D. (2003) Calcium-induced calcium release. Curr. Biol. **13**, R425

14 Galione, A. and Chuang, K. T. (2012) Pyridine nucleotide metabolites and calcium release from intracellular stores. Adv. Exp. Med. Biol. **740**, 305–323

15 Cosker, F., Cheviron, N., Yamasaki, M., Menteyne, A., Lund, F. E., Moutin, M. J., Galione, A. and Cancela, J. M. (2010) The ecto-enzyme CD38 is a nicotinic acid adenine dinucleotide phosphate (NAADP) synthase that couples receptor activation to Ca^{2+} mobilization from lysosomes in pancreatic acinar cells. J. Biol. Chem. **285**, 38251–38259

16 Aarhus, R., Dickey, D. M., Graeff, R. M., Gee, K. R., Walseth, T. F. and Lee, H. C. (1996) Activation and inactivation of Ca^{2+} release by $NAADP^+$. J. Biol. Chem. **271**, 8513–8516

17 Churchill, G. C. and Galione, A. (2001) NAADP induces Ca^{2+} oscillations via a two-pool mechanism by priming IP₃- and cADPR-sensitive Ca^{2+} stores. EMBO J. **20**, 2666–2671

18 Churchill, G. C., Okada, Y., Thomas, J. M., Genazzani, A. A., Patel, S. and Galione, A. (2002) NAADP mobilizes Ca^{2+} from reserve granules, lysosome-related organelles, in sea urchin eggs. Cell **111**, 703–708

19 Galione, A., Morgan, A. J., Arredouani, A., Davis, L. C., Rietdorf, K., Ruas, M. and Parrington, J. (2010) NAADP as an intracellular messenger regulating lysosomal calcium-release channels. Biochem. Soc. Trans. **38**, 1424–1431

20 Ishibashi, K., Suzuki, M. and Imai, M. (2000) Molecular cloning of a novel form (two-repeat) protein related to voltage-gated sodium and calcium channels. Biochem. Biophys. Res. Commun. **270**, 370–376

21 Calcraft, P. J., Ruas, M., Pan, Z., Cheng, X., Arredouani, A., Hao, X., Tang, J., Rietdorf, K., Teboul, L., Chuang, K. T. et al. (2009) NAADP mobilizes calcium from acidic organelles through two-pore channels. Nature **459**, 596–600

22 Patel, S., Marchant, J. S. and Brailoiu, E. (2010) Two-pore channels: regulation by NAADP and customized roles in triggering calcium signals. Cell Calcium **47**, 480–490

23 Brailoiu, E., Churamani, D., Cai, X., Schrlau, M. G., Brailoiu, G. C., Gao, X., Hooper, R., Boulware, M. J., Dun, N. J., Marchant, J. S. and Patel, S. (2009) Essential requirement for two-pore channel 1 in NAADP-mediated calcium signaling. J. Cell Biol. **186**, 201–209

24 Aley, P. K., Mikolajczyk, A. M., Munz, B., Churchill, G. C., Galione, A. and Berger, F. (2010) Nicotinic acid adenine dinucleotide phosphate regulates skeletal muscle differentiation via action at two-pore channels. Proc. Natl. Acad. Sci. U.S.A. **107**, 19927–19932

25 Zhu, M. X., Ma, J., Parrington, J., Calcraft, P. J., Galione, A. and Evans, A. M. (2010) Calcium signaling via two-pore channels: local or global, that is the question. Am. J. Physiol. Cell. Physiol. **298**, C430–C441

26 Luzio, J. P., Pryor, P. R. and Bright, N. A. (2007) Lysosomes: fusion and function. Nat. Rev. Mol. Cell Biol. **8**, 622–632

27 Holt, O. J., Gallo, F. and Griffiths, G. M. (2006) Regulating secretory lysosomes. J. Biochem. **140**, 7–12

28 Schroder, B. A., Wrocklage, C., Hasilik, A. and Saftig, P. (2010) The proteome of lysosomes. Proteomics **10**, 4053–4076

29 Nagai, T., Yamada, S., Tominaga, T., Ichikawa, M. and Miyawaki, A. (2004) Expanded dynamic range of fluorescent indicators for Ca^{2+} by circularly permuted yellow fluorescent proteins. Proc. Natl. Acad. Sci. U.S.A. **101**, 10554–10559

30 Scherer, W. F., Syverton, J. T. and Gey, G. O. (1953) Studies on the propagation in vitro of poliomyelitis viruses. IV. Viral multiplication in a stable strain of human malignant epithelial cells (strain HeLa) derived from an epidermoid carcinoma of the cervix. J. Exp. Med. **97**, 695–710

31 Haynes, L. P., Tepikin, A. V. and Burgoyne, R. D. (2004) Calcium-binding protein 1 is an inhibitor of agonist-evoked, inositol 1,4,5-trisphosphate-mediated calcium signaling. J. Biol. Chem. **279**, 547–555

32 Diarra, A., Wang, R., Garneau, L., Gallo-Payet, N. and Sauve, R. (1994) Histamine-evoked Ca^{2+} oscillations in HeLa cells are sensitive to methylxanthines but insensitive to ryanodine. Pflügers Arch. **426**, 129–138

33 Esposito, B., Gambara, G., Lewis, A. M., Palombi, F., D'Alessio, A., Taylor, L. X., Genazzani, A. A., Ziparo, E., Galione, A., Churchill, G. C. and Filippini, A. (2011) NAADP links histamine H1 receptors to secretion of von Willebrand factor in human endothelial cells. Blood **117**, 4968–4977

34 Michelangeli, F. and East, J. M. (2011) A diversity of SERCA Ca^{2+} pump inhibitors. Biochem. Soc. Trans. **39**, 789–797

35 Naylor, E., Arredouani, A., Vasudevan, S. R., Lewis, A. M., Parkesh, R., Mizote, A., Rosen, D., Thomas, J. M., Izumi, M., Ganesan, A. et al. (2009) Identification of a chemical probe for NAADP by virtual screening. Nat. Chem. Biol. **5**, 220–226

36 Berg, T. O., Stromhaug, E., Lovdal, T., Seglen, O. and Berg, T. (1994) Use of glycyl-L-phenylalanine 2-naphthylamide, a lysosome-disrupting cathepsin C substrate, to distinguish between lysosomes and prelysosomal endocytic vacuoles. Biochem. J. **300**, 229–236

37 McCue, H. V., Burgoyne, R. D. and Haynes, L. P. (2011) Determination of the membrane topology of the small EF-hand Ca^{2+}-sensing proteins CaBP7 and CaBP8. PLoS ONE **6**, e17853

38 LaFerla, F. M. (2002) Calcium dyshomeostasis and intracellular signalling in Alzheimer's disease. Nat. Rev. Neurosci. **3**, 862–872

39 Surmeier, D. J. (2007) Calcium, ageing, and neuronal vulnerability in Parkinson's disease. Lancet Neurol. **6**, 933–938

40 Lim, D., Fedrizzi, L., Tartari, M., Zuccato, C., Cattaneo, E., Brini, M. and Carafoli, E. (2008) Calcium homeostasis and mitochondrial dysfunction in striatal neurons of Huntington disease. J. Biol. Chem. **283**, 5780–5789

41 Beuckelmann, D. J., Nabauer, M. and Erdmann, E. (1992) Intracellular calcium handling in isolated ventricular myocytes from patients with terminal heart failure. Circulation **85**, 1046–1055

42 Rizzuto, R. and Pozzan, T. (2003) When calcium goes wrong: genetic alterations of a ubiquitous signaling route. Nat. Genet. **34**, 135–141

43 Haller, T., Dietl, P., Deetjen, P. and Volkl, H. (1996) The lysosomal compartment as intracellular calcium store in MDCK cells: a possible involvement in InsP₃-mediated Ca^{2+} release. Cell Calcium **19**, 157–165

44 Patel, S. and Docampo, R. (2010) Acidic calcium stores open for business: expanding the potential for intracellular Ca^{2+} signaling. Trends Cell Biol. **20**, 277–286

45 Morgan, A. J., Platt, F. M., Lloyd-Evans, E. and Galione, A. (2011) Molecular mechanisms of endolysosomal Ca^{2+} signalling in health and disease. Biochem. J. **439**, 349–374

46 Lloyd-Evans, E. and Platt, F. M. (2011) Lysosomal Ca^{2+} homeostasis: role in pathogenesis of lysosomal storage diseases. Cell Calcium **50**, 200–205

47 Miyawaki, A., Llopis, J., Heim, R., McCaffery, J. M., Adams, J. A., Ikura, M. and Tsien, R. Y. (1997) Fluorescent indicators for Ca^{2+} based on green fluorescent proteins and calmodulin. Nature **388**, 882–887

48 Emmanouilidou, E., Teschemacher, A. G., Pouli, A. E., Nicholls, L. I., Seward, E. P. and Rutter, G. A. (1999) Imaging Ca^{2+} concentration changes at the secretory vesicle surface with a recombinant targeted cameleon. Curr. Biol. **9**, 915–918

49 Putney, J. W. (2011) Origins of the concept of store-operated calcium entry. Front. Biosci., Scholar Ed. **3**, 980–984

50 Handley, M. T., Lian, L. Y., Haynes, L. P. and Burgoyne, R. D. (2010) Structural and functional deficits in a neuronal calcium sensor-1 mutant identified in a case of autistic spectrum disorder. PLoS ONE **5**, e10534

51 Tian, L., Hires, S. A., Mao, T., Huber, D., Chiappe, M. E., Chalasani, S. H., Petreanu, L., Akerboom, J., McKinney, S. A., Schreiter, E. R. et al. (2009) Imaging neural activity in worms, flies and mice with improved GCaMP calcium indicators. Nat. Methods **6**, 875–881

52 Shen, D., Wang, X., Li, X., Zhang, X., Yao, Z., Dibble, S., Dong, X. P., Yu, T., Lieberman, A. P., Showalter, H. D. and Xu, H. (2012) Lipid storage disorders block lysosomal trafficking by inhibiting a TRP channel and lysosomal calcium release. Nat. Commun. **3**, 731

53 Demaurex, N. and Frieden, M. (2003) Measurements of the free luminal ER Ca^{2+} concentration with targeted "cameleon" fluorescent proteins. Cell Calcium **34**, 109–119